In: Wagner W., Székely, B. (eds.): ISPRS TC VII Symposium – 100 Years ISPRS, Vienna, Austria, July 5–7, 2010, IAPRS, Vol. XXXVIII, Part 7B

Contents   Author Index   Keyword Index

URBAN VEGETATION DETECTION USING HIGH DENSITY FULL-WAVEFORM AIRBORNE LIDAR DATA - COMBINATION OF OBJECT-BASED IMAGE AND POINT CLOUD ANALYSIS

B. Höfle [a, *], M. Hollaus [b]

[a] University of Heidelberg, Department of Geography, 69120 Heidelberg, Germany - hoefle@uni-heidelberg.de
[b] Vienna University of Technology, Institute of Photogrammetry and Remote Sensing, 1040 Vienna, Austria - mh@ipf.tuwien.ac.at

KEY WORDS: Airborne LiDAR, Vegetation mapping, Open source GIS, Object-Based Image Analysis

ABSTRACT:

In this paper, a new GIS workflow for fully automated urban vegetation and tree parameter extraction from airborne LiDAR data is presented. The strengths of both raster- and point cloud-based methods are combined, in order to derive a vegetation map layer as well as single tree parameters (e.g. tree height and crown width) in an efficient way. The workflow is implemented in GRASS GIS making use of standard GIS functionality and newly developed tools providing access to point cloud analysis. An edge-based segmentation delineates potential tree crowns, which are further aggregated to single trees or group of trees by using local topological information (e.g. percentage of outline touched by neighbors) and constraints on segment geometry (e.g. shape of segments). Furthermore, the classification makes use of segment attributes that have been extracted from the full-waveform point cloud (e.g. percentage of first echoes, echo width and signal amplitude). A representative study area in the City of Vienna is used to demonstrate the applicability of the developed object-based GIS workflow. Buildings and vegetation objects could be separated with high accuracy, where at maximum 14% of classified vegetation segments confuse with buildings (mainly building edges). Concluding, the unique high density (50 pts/m^2) full-waveform LiDAR data open a new scale in 3D object extraction but demanding for novel strategies in object-based raster and point cloud analysis.

1. INTRODUCTION

Vegetation monitoring and tree inventory play an important role in modern urban spatial data management, as many benefits and applications inherit from this detailed up-to-date data source such as monitoring of functions (e.g. noise and pollution mitigation) and creation of 3D city models (Vosselman, 2003). Compared to predominant studies on vegetation detection and characterization mainly in purely forested areas (e.g. Hyyppä et al., 2001), this study concentrates on urban areas, which have a high structural complexity with a multitude of different objects (e.g. temporary objects, vegetation on top of buildings, road signs, power lines and cables). Previous studies using airborne LiDAR for vegetation and single tree detection, respectively, used image-based methods, e.g. including orthophotos (Hirschmugl et al., 2007; Iovan et al., 2007; Secord and Zakhor, 2007) and derived raster layers e.g. first-last-pulse difference (Liang et al., 2007). Novel approaches include full-waveform (FWF) information (e.g. echo width and amplitude) for urban object detection in the 3D point cloud directly (Mallet et al., 2008; Rutzinger et al., 2007 and 2008) and for 3D segmentation of single trees (Reitberger et al., 2009).

Höfle et al. (2008) showed the suitability of aggregated FWF attributes attached to segments derived from image analysis for tree species discrimination. This paper aims at transferring this combined object-based image (Blaschke, 2010) and point cloud analysis from forested to complex urban areas, in order to derive a GIS-ready vegetation mask. To date, high point density (~50 echoes/m^2) LiDAR data are increasingly available in particular for urban areas. This high point density does not allow to apply computationally intensive 3D point cloud analysis in an operational manner, which is a prerequisite for being used in city map and cadastre generation. Thus, this study presents a novel GIS framework for full-waveform LiDAR data land cover classification, making use of both image and point cloud analysis (cf. Höfle et al., 2009).

2. STUDY AREA AND DATASETS

The study area is located in the city centre of Vienna, Austria, and comprise the three city parks: Rathauspark, Volksgarten and Burggarten (Fig. 1). A great variety of planting and tree species can be found within the test site, e.g. alley of trees, short-cut trees, hedgerows and shrubs. Deciduous trees are predominant, e.g. beech (*Fagus sylvatica*), Norway maple (*Acer platanoides*), plane (*Platanus acerifolia*), linden (*Tilia cordata, platyphyllos*) and chestnut (*Aesculus hippocastanum*) and sparsely coniferous species. The area is characterized by large building complexes (e.g. city hall, Burgtheater and parliament). Furthermore, artificial objects such as fences, cars, power lines, park benches as well as a high amount of people are usually present in this central part of the city, and therefore also included in the airborne LiDAR elevation datasets.

---

* Corresponding author.

In: Wagner W., Székely, B. (eds.): ISPRS TC VII Symposium – 100 Years ISPRS, Vienna, Austria, July 5–7, 2010, IAPRS, Vol. XXXVIII, Part 7B

Contents   Author Index   Keyword Index

Figure 1. Study area located in the city centre of Vienna, Austria. Diversity in tree species and structure are shown in detailed photographs (B1-B3)

The full-waveform airborne LiDAR data were obtained in the framework of the city-wide laser scanning campaign in the winter season 2006/2007 under leaf-off conditions. Data acquisition was performed with a Riegl LMS-Q560 system, which uses near-infrared (1500 nm) laser pulses with a pulse width of 4 ns. Further settings are a pulse repetition frequency of 200 kHz, scan angle range of ±22.5° and a beam divergence of 0.5 mrad. Full-waveform recording can be done with 1 ns temporal resolution. Decomposition of the waveforms was performed by using the Riegl software RiANALYZE. The number of echoes is not limited by the full-waveform recording sensor system, and therefore, the number of detected echoes per laser shot can be higher as with traditional discrete echo recording, particularly in high vegetation. The average echo density of the LiDAR dataset covering the study area is 50 echoes per m^2 with about 6.8% first echoes, 1% intermediate echoes (e.g. 2nd, 3rd echo), 6.8% last and 85.4% single echoes (i.e. only one reflection per shot). A Digital Terrain Model (DTM) with 0.5 m resolution was produced using the software SCOP++ (SCOP++, 2010). For evaluation and comparison a reference dataset including single tree positions of alley trees as well as the official land cover map of Vienna are available: Mehrzweckkarte (MZK), Flächenmehrzweckkarte[1] (FMZK).

3. METHODS

The very high point density of the LiDAR dataset, i.e. about $50 \cdot 10^6$ echoes per km^2, does not allow a pure point cloud based vegetation detection procedure for large areas ($400 \ km^2$ for entire Vienna) in an operational manner. Therefore, a combined object-based image and point cloud approach is introduced, taking advantage of both, fast raster processing and detailed ("interpolation-free") point cloud based information extraction including full-waveform laser point attributes. Furthermore, the high point density of the point cloud allows the derivation of high-resolution derivatives (e.g. DTM with 0.5 m cell size), providing a sufficient planimetric accuracy of the final results.

[1] http://www.wien.gv.at/stadtentwicklung/stadtvermessung/geod aten/fmzk/produkt.html (last accessed 31.5.2010)

The developed workflow is implemented in the GRASS GIS environment (GRASS Development Team, 2010) and comprises the steps shown in Fig. 2.
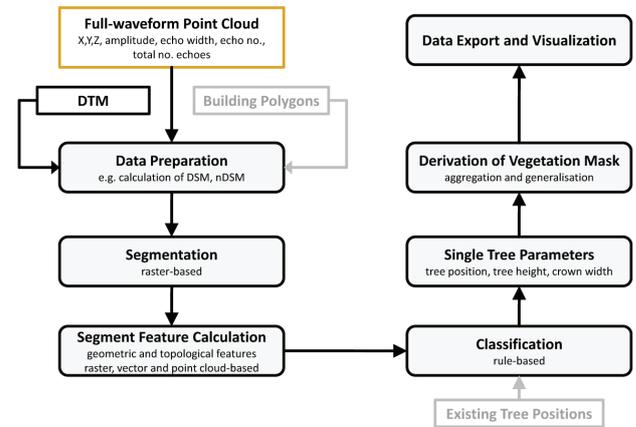

Figure 2. Workflow of urban vegetation detection using raster and full-waveform point cloud input data

3.1 Data preparation

The data preparation of the input point cloud ASCII file includes a classification of the laser points into first, last, single and intermediate echoes. Each laser point has the attributes echo number (EN) and total number (TN) of echoes of the corresponding laser shot, with e.g. single echoes: EN=TN=1; first echoes: EN=1 && TN>1; intermediate echoes: EN>1 && EN!=TN. Using the maximum height per 0.5 m cell a Digital Surface Model (DSM) is derived and finally normalized with the input DTM, in order to get a normalized DSM (nDSM). Empty cells get a normalized height of 0 m. In urban areas generally complete and high quality cadastral data layers are available, which can be used as mask for the subsequent steps.
In our study the buildings can be extracted from the official land cover map and could be used optionally to exclude these areas from further investigation. In our study the building polygons are used for evaluation and thus are not considered as input.

3.2 Segmentation

An object-based raster analysis using an edge-based segmentation procedure is applied to the high-resolution nDSM. The procedure has already been tested in densely forested areas where no buildings are present (Höfle et al., 2008) and is transferred to the densely built-up urban area of Vienna in this study. The segmentation aims at delineating convex objects in the nDSM by finding concave edges in between the objects. Additionally, constraints on normalized height (nDSM>1.0 m) and the occurrence of multiple reflections are included. Multiple reflections are parametrized by an echo ratio (ER) defined as (Eq. 1):

$$ER \ [\%] = (n_{first} + n_{intermediate}) \ / \ (n_{last} + n_{single}) \cdot 100 \qquad (1)$$

where n is the respective number of echoes per cell. If no echo is within a cell, ER is set to zero and if no last and single echoes are found within a cell, the echo ratio is set to 100, exhibiting a high vertical extension and transparency of the object. High ER values are assumed to indicate vegetation, which tends to have a high number of first and intermediate echoes compared to other elevated objects in urban areas (e.g. buildings; Fig. 3b).

In: Wagner W., Székely, B. (eds.): ISPRS TC VII Symposium – 100 Years ISPRS, Vienna, Austria, July 5–7, 2010, IAPRS, Vol. XXXVIII, Part 7B

Contents　　　　　　　　　Author Index　　　　　　　　　Keyword Index

The edge detector is based on applying a threshold to the minimum curvature in direction perpendicular to the direction of maximum curvature in a certain window (e.g. 7x7 cells), i.e. curvature<0.0 for concave areas (cf. Fig. 3c), and skeletonizing the potential edge areas to reach a final edge map. These edges correspond to the segment boundaries between adjacent objects. By combining the edge map with areas fulfilling height (e.g. >1.0 m; Fig. 3a) and ER threshold (e.g. >5%; Fig. 3b), the final segment raster is derived. In order to derive the segment polygons, a connected component labeling and vectorization of the connected region boundaries are applied (Fig. 3d).
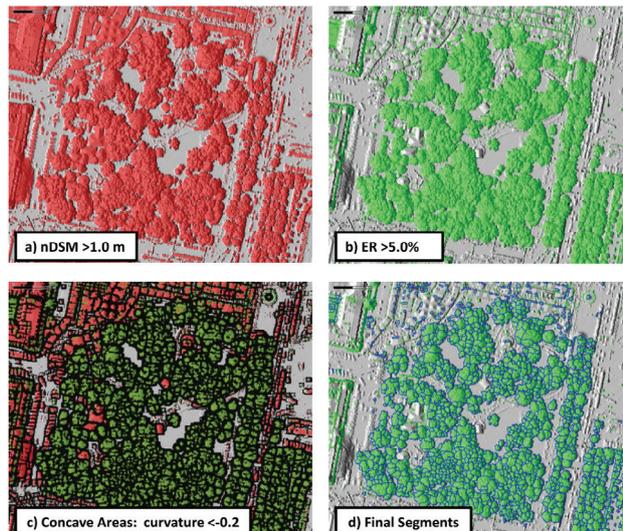

Figure 3. Input layers for segmentation of convex regions in the nDSM having high transparency (i.e. echo ratio)

3.3 Segment feature calculation

For classification of the derived segments the available segment features (i.e. attributes attached to the segment polygons) are essential. In this step an extensive segment feature database is generated, considering segment features based on the point cloud, segment geometry and topology (Fig. 4). The derived features are attached to the attribute table of the GIS polygon layer. By Point-in-Polygon-Test the point attributes (normalized height, amplitude, echo width) stratified by laser echo classes (all, first, multi echoes = first and intermediate, last and single) are aggregated (number of echoes, min., mean, max., standard deviation) per point attribute and segment. In this aggregation step the laser echoes are filtered by the minimum vegetation height value of 1 m above ground, in order to exclude the terrain signature from the segment statistics, except the descriptive statistics for the "all" echo class. Additionally, the number of points falling within a potential height interval for tree stems (i.e. between 1.0 m and 2.5 m) are counted per segment. Furthermore, the ER on segment basis is derived (Eq. 1), and the percentage of points below the minimum vegetation height (i.e. 1.0 m) and above are attached. To include surface information, the statistics of the nDSM cell values are also calculated per segment (e.g. mean nDSM height). Based on segment polygon geometry i) area, ii) perimeter, iii) compactness (perimeter / (2 * sqrt(π * area)) are derived. Due to the topological vector data model in GRASS GIS, topological information can easily be assessed and attached to the segments: i) number of adjacent polygons and ii) percentage of boundary shared with neighbors. All together 66

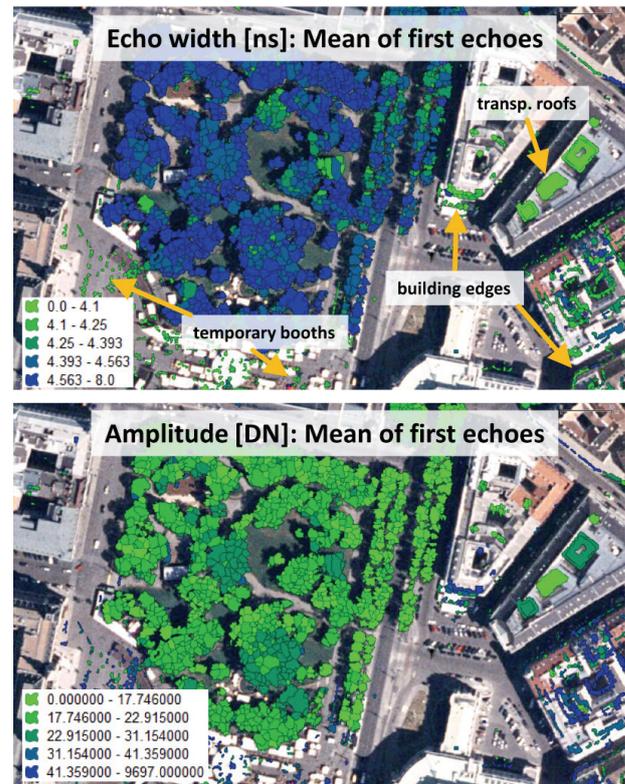segment features could be obtained for each segment with 53 point cloud based values.

Figure 4. Segments colored by mean echo width (top) and signal amplitude (bottom) of all first echoes within a segment. Non-vegetation segments can clearly be identified by low echo widths and higher amplitudes

3.4 Classification

Exploratory data analysis was performed, in order to set-up a rule-base for supervised classification. A logical rule base for classification was developed, which in a first step aims at separating vegetation from non-vegetation segments. Tree positions from the reference map are included in the classification process. Final classes and classification hierarchy are shown in Fig. 5. The GIS environment easily allows to perform the final classification using SQL statements in the attribute database.
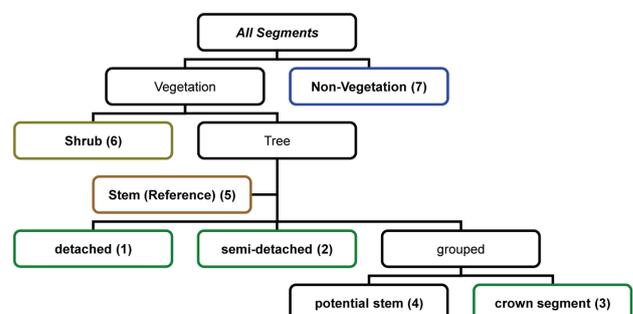

Figure 5. Classification scheme including reference tree positions. Target classes are numbered from 1 to 7.

In: Wagner W., Székely, B. (eds.): ISPRS TC VII Symposium – 100 Years ISPRS, Vienna, Austria, July 5–7, 2010, IAPRS, Vol. XXXVIII, Part 7B

Contents   Author Index   Keyword Index

3.5 Tree segment parameters

The city administration is mainly interested in updating tree parameters for their available tree positions. These parameters serve for the city tree inventory but also for visualization purposes (i.e. virtual reality/city). Tree position, tree height and crown diameter are derived for the classified stem and potential stem segments. Due to the occurrence of power lines, adjacent buildings/roofs a robust calculation of tree height is introduced. The robust tree height is defined as the highest laser point fulfilling the criterion of being within a maximum height above the mean height of the k highest points of a segment (Fig. 6a). Tree crown diameter is approximated by the smallest enclosing circle (SEC) to the segment boundary including calculation of the mean deviation to the maximum diameter, in order to provide a quality measure of the derived diameter value (Fig. 6b). Different methods for tree position estimation are implemented: i) position of robust highest point, ii) circle center of SEC, iii) center of gravity of segment boundary vertices (Fig. 6c). The tree position estimation results in a new point GIS vector layer holding all segment attributes as well as crown diameter and tree height attributes.
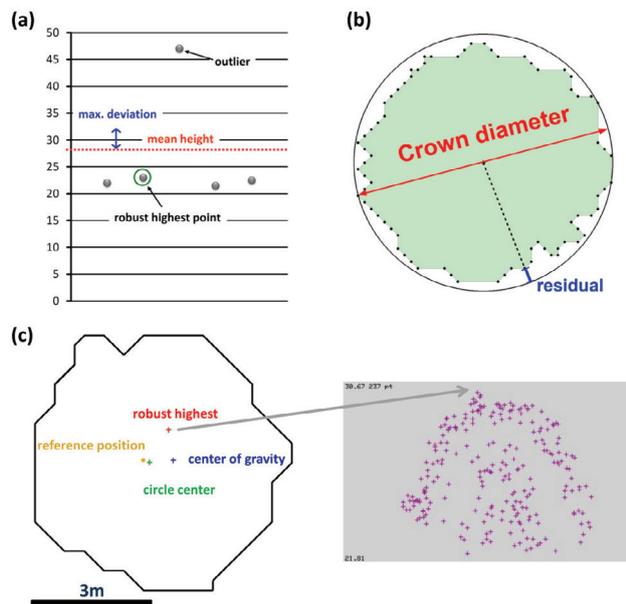

Figure 6. (a) Robust highest point/segment, (b) crown diameter by smallest enclosing circle and (c) different methods of tree position estimation compared with reference position (left) and point cloud cross-section indicating highest point (right)

3.6 Derivation of vegetation mask

Vegetation mask derivation is straightforward, due to the GIS vector topology. Common boundaries between vegetation segments are dissolved, i.e. adjacent polygons are merged. This procedure is followed by a generalization step, where small isolated polygons are removed (e.g. 20 m^2) and small holes (i.e. islands; e.g. 20 m^2) are closed. Furthermore, the vegetation mask boundary can be generalized by line simplification (e.g. Douglas-Peucker) or smoothing (e.g. Snakes) readily available in the GRASS GIS framework.

4. RESULTS AND DISCUSSION

The defined echo ratio (ER) raster layer based on echo classes (e.g. first, last echo) clearly shows a very good agreement with potential urban vegetation areas (Fig. 3b). Compared to other definitions of echo ratios, such as a purely geometric computation (e.g. Rutzinger et al., 2007; Höfle et al., 2009) where number of neighbors are counted in a defined 2D and 3D neighborhood, the high point density and the increased echo detection sensitivity and echo labeling provided by full-waveform LiDAR allows this faster ER derivation without the need for computationally intensive 3D point cloud neighborhood analysis. Furthermore, the full-waveform based ER is more robust against multi-temporal effects caused by temporary objects (Fig. 7). For example, a truck scanned in one flight strip but not present in a second strip covering the same area will cause an artificial object with a certain height above terrain and a very high transparency but will still have low echo widths and a low number of multiple echoes per shot.
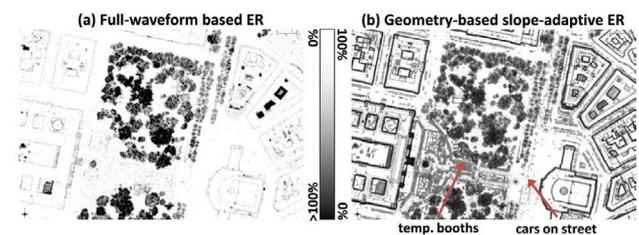

Figure 7. (a) Full-waveform based echo ratio (ER), (b) geometry-based echo ratio (Höfle et al., 2009). Temporary objects can clearly be identified in the geometry-based ER

In order to evaluate the separation capability of vegetation from non-vegetation, the optional building mask was not included for segmentation. Our experiments have shown that optional including of a building mask achieves best results when used as "soft mask", due to the occurrence of buildings below vegetation such as smaller buildings in parks or subway stations below alley trees. A "hard mask" would exclude building areas found in the cadastre from further processing and thus finally classify these areas as non-vegetation. A soft mask means a stricter threshold on ER than for the non-building areas (e.g. ER>50%), which should exclude most of structures related to free-standing buildings (e.g. walls and antennas) but still enables the detection of vegetation overtopping low buildings. These trees are mainly deciduous species and hence transparent under leaf-off conditions with a high number of laser shots with multiple echoes (i.e. high ER). The choice of window size for curvature calculation controls the degree of detail reflected in over- or under-segmentation (cf. Höfle et al., 2008). The larger the window size, the less segments are found. The threshold on curvature additionally controls the sensitivity for edge detection. The more moderate the threshold is chosen, the more edges can be detected, but also the potential edge zones become wider (Fig. 3c) and thus the location accuracy of the "thinned" edge line gets more uncertain. The location accuracy of the depression line between two objects could be improved by weighted skeletonization (by curvature and height) or drawing profiles for detecting the lowest point or the point with highest concavity in the boundary zone of two segments.

The segmentation step results in 23788 segments (compared to 67 Mio. laser echoes within the study site) with an average size of 10.6 m^2. A window size of 7x7 pixel (i.e. 0.5 m resolution) for curvature calculation with curvature constraint of lower than -0.2 were chosen. Trees with a compact and convex crown

In: Wagner W., Székely, B. (eds.): ISPRS TC VII Symposium – 100 Years ISPRS, Vienna, Austria, July 5–7, 2010, IAPRS, Vol. XXXVIII, Part 7B

Contents　　　　　　　　　Author Index　　　　　　　　　Keyword Index

shape result in one segment, whereas large deciduous trees with multiple tree tops are represented by multiple segments (one per convex tree top). For selected 181 alley trees the average number of segments per tree is 2.6, indicating over-segmentation and trees with multiple tops, respectively. Within the park areas with larger deciduous trees the number of segments per tree lies clearly higher but could not be assessed due to missing reference positions. Over-segmentation can also be reduced by prior filtering (e.g. Gauss filter) of the DSM in order to reduce canopy roughness and suppress small structures (cf. Hirschmugl et al., 2007).

7 - Non-Vegetation	
Perc. of echoes above min. height (2 m) [%]	>99.0
Mean amplitude of first echoes [DN]	>50
Mean amplitude of last echoes [DN]	>100
Mean echo width of first echoes [ns]	< 4.1
Std.dev. of echo width of first echoes [ns]	< 0.35
Std.dev. of heights of first echoes [m]	> 10
Std.dev. of heights of first echoes [m]	< 0.2
ER of segment [%]	< 5
Compactness &&	> 1.7
Mean nDSM height [m] &&	> 3.0
Stddev. of height of first echoes &&	≥ 1.0
Perc. of boundary covered by neighbors	< 60%
6 - Shrubs	
Mean nDSM height [m] &&	< 3.0
Std.dev. of heights of first echoes [m]	< 1.0
5 - Stem (reference)	
Distance to reference tree position [m]	< 1.0
1 - Detached	
No. of adjacent segments	≤ 0
2 - Semi-detached	
Perc. of boundary covered by neighbors	< 20
4 - Potential stem segment	
Number of echoes in height interval 1.0 - 2.5 m	> 10
3 - Crown segment	
All remaining segments	

Table 1. Rules and thresholds on segment attributes for detecting vegetation and further characterization

Although the constraint on ER already excluded the majority of non-vegetation objects, the segments still contain non-vegetation objects such as building walls, roof overhangs, transparent roofs and power lines. Thus, full-waveform point cloud information derived on segment level is valuable for separating vegetation from non-vegetation. Particularly, echo width and signal amplitude show clear signatures for vegetation (refer to Fig. 4). Vertically extended objects with a multitude of small scatterers (e.g. branches) exhibit larger echo widths and lower amplitudes due to the relatively small target areas contributing to each echo (cf. Wagner et al., 2008). The main part is to exclude non-vegetation segments. Through exploratory data analysis and visual inspection suitable attributes and thresholds could be obtained. Table 1 shows the applied rules to the rule base defined in Fig. 5 and Fig. 8 the resulting classified segments. For example, the percentage of echoes above the min. tree height of 1 m indicates a low ground penetration, which mainly occurs at building walls not connected with the ground, transparent roofs, antennas on roofs, and even vegetation on top of buildings, exhibiting an ER above 5%. Building facades can be excluded by high compactness, as they are elongated, and high std.dev. of first echo heights together with low coverage of adjacent segments and relatively high mean nDSM heights. High nDSM heights

for vertical walls are also due to the generation procedure of the DSM, where the maximum height value per cell is taken. Shrubs are distinguished by using mean nDSM height and std.dev. of first echo heights, which is assumed to be lower than for trees.
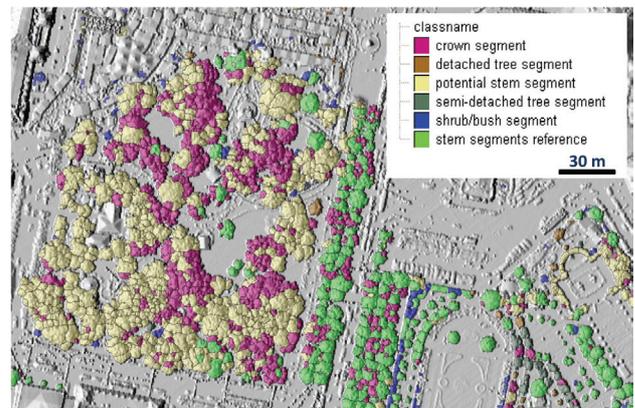

Figure 8. Classified vegetation segments further separated into six sub-classes.

This manual set up and selection of attributes and thresholds will be replaced by automatic classification procedures in future such as statistical classification trees (Rutzinger et al., 2008) or Support Vector Machines (Mallet et al., 2008), which have already been applied to classify single laser points of large point clouds. The segment-based approach may lead to more stable features for classification (e.g. mean echo width per segment; cf. Rutzinger et al., 2008) but is strongly dependent on the quality and delineation accuracy of the segmentation. The current state of segmentation and classification provides the necessary input for vegetation mask generation and derivation of tree segment parameters (e.g. height, diameter, position) for visualization purposes by reconstructing artificial tree objects (cf. Vosselman, 2003). However, for urban tree inventory single tree detection is required and tree positions should be derived from stem detection. The class of potential stem segments could be a starting point for further point cloud based stem extraction. Multi-level/scale segmentation, i.e. further segmentation on the derived segments, could solve the problem of over-segmentation (Blaschke, 2010) and join segments belonging to one tree. Promising studies have already shown the potential of point cloud based single tree detection for airborne (Reitberger et al., 2009) and mobile LiDAR data (Rutzinger et al., 2010). No point cloud segmentation is required for the class of detached tree segments, representing a single tree object. But for trees with multiple tops and no distinct crown shape 3D point cloud segmentation shows great potential, providing the required information inherent in the vertical sampling of the objects by airborne LiDAR. Multi-level LiDAR analysis, such as prior image based detection of candidate regions with following point cloud based object detection increasing delineation and classification accuracy offers the possibility to process large areas even with very high point densities in an operational manner without major loss in classification accuracy, if the pre-selection has high completeness (cf. Höfle et al., 2009).

For evaluation the alley tree inventory (i.e. tree positions) is used. Out of 668 alley trees 639 (95.7%) could be successfully detected and included in the final vegetation mask. The missing trees are mainly young trees with low diameter and crown area,

In: Wagner W., Székely, B. (eds.): ISPRS TC VII Symposium – 100 Years ISPRS, Vienna, Austria, July 5–7, 2010, IAPRS, Vol. XXXVIII, Part 7B

Contents   Author Index   Keyword Index

below the defined minimum segment area of 2 m^2. Confusion with buildings (mainly the edges) is the major task of separating vegetation in urban areas. Using the cadastral building layer 3.4% of the total vegetation segment area intersects with buildings and 7.7%, if the building polygons are buffered with 2 m, indicating that predominantly building edges are wrongly classified. Note that also buildings overtopped by vegetation are also counted as error. On segment basis 4.8% of segments (402 of 8413) are intersecting with buildings with more than 50% of their area. Looking at the buffered buildings, 14.0% (1182) of the segments confuse with building areas.
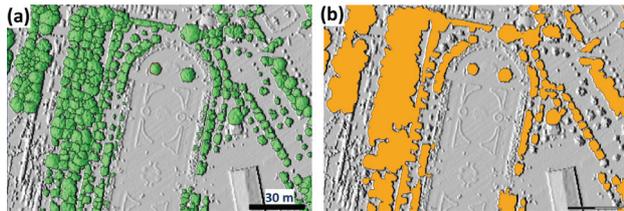

Figure 9. (a) Vegetation segments and (b) derived generalized vegetation GIS layer

The final result is the generalized vegetation mask (Fig. 9), generated by using the segments falling within one of the vegetation classes. Generalization was performed by removing small isolated vegetation areas (<20 m^2) and holes within vegetation (<20 m^2). Additionally the vegetation layer boundary is smoothed using Snakes (α=1.0).

5. CONCLUSIONS

This paper presented a novel workflow of GIS-based urban vegetation mapping using high density full-waveform LiDAR data. The combination of image-based object analysis and point cloud-based segment feature derivation and classification shows promising results for automated, operational applications, such as urban mapping, map updating, 3D visualization and urban tree inventory, when combined with single tree and stem detection algorithms. Future work will concentrate on including radiometric calibration, automated classification (e.g. statistical decision trees) and point cloud based single tree detection.

ACKNOWLEDGMENTS

REFERENCES

Blaschke, T., 2010. Object based image analysis for remote sensing. *ISPRS Journal of Photogrammetry and Remote Sensing*, 65, pp. 2-16.

GRASS Development Team, 2010. Geographic Resources Analysis Support System (GRASS) Software, Version 6.4.0. Open Source Geospatial Foundation. http://grass.osgeo.org

Hirschmugl, M., Ofner, M., Raggam, J., Schardt, M., 2007. Single tree detection in very high resolution remote sensing data. *Remote Sensing of Environment*, 110, pp. 533-544.

Höfle, B., Hollaus, M., Lehner, H., Pfeifer, N., Wagner, W., 2008. Area-based parameterization of forest structure using full-waveform airborne laser scanning data. In: *Proc. Silvilaser 2008*, Edinburgh, Scotland, pp. 227-235.

Höfle, B., Mücke, W., Dutter, M., Rutzinger, M. , Dorninger, P., 2009. Detection of building regions using airborne LiDAR - A new combination of raster and point cloud based GIS methods. In: *Proc. of the GI_Forum*, Salzburg, pp. 66-75.

Hyyppä, J., et al., 2001, HIGH-SCAN: The first European-wide attempt to derive single-tree information from laserscanner data. *The Photogrammetric Journal of Finland*, 17, pp. 58-68.

Iovan, C., Boldo, D., Cord, M, 2007. Automatic extraction of urban vegetation structures from high resolution imagery and digital elevation model. In: *Urban Remote Sensing Joint Event, URBAN 2007 – URS 2007*, Paris, pp. 1-5.

Liang, X., J. Hyyppä, J., Matikainen, L., 2007. Deciduous-coniferous tree classification using difference between first and last pulse laser signatures. In: *IAPRS*, Vol. 36, Part 3/W52, pp. 253-257.

Mallet, C., Bretar, F., Soergel, U., 2008. Analysis of Full-waveform LiDAR Data for Classification of Urban Areas. *Photogrammetrie Fernerkundung Geoinformation*, 5, pp. 337-349.

Reitberger, J., Schnörr, C., Krzystek, P., Stilla, U., 2009. 3D segmentation of single trees exploiting full waveform LIDAR data. *ISPRS Journal of Photogrammetry and Remote Sensing*, 64, pp. 561-574.

Rutzinger, M., Höfle, B., Pfeifer, N., 2007. Detection of high urban vegetation with airborne laser scanning data. In: *Proceedings Forestsat 2007*. Montpellier, France, pp. 1-5.

Rutzinger, M., Höfle, B., Hollaus, M., Pfeifer, N., 2008. Object-Based Point Cloud Analysis of Full-Waveform Airborne Laser Scanning Data for Urban Vegetation Classification. *Sensors*, 8(8), pp. 4505-4528.

Rutzinger, M., Pratihast, A.K., Oude Elberink, S., Vosselman, G., 2010. Detection and Modeling of 3D Trees from Mobile Laser Scanning Data. In: *Proc. ISPRS TCV Mid-Term Symposium*, Newcastle upon Tyne, 6p.

Secord, J., Zakhor, A., 2007. Tree Detection in Urban Regions Using Aerial Lidar and Image Data. *IEEE Geoscience and Remote Sensing Letters*, 4(2), pp. 196-200.

SCOP++, 2010. Institute of Photogrammetry and Remote Sensing, www.ipf.tuwien.ac.at/products/products.html, last accessed 31.05.2010.

Vosselman, G., 2003. 3D reconstruction of roads and trees for city modelling. In. *IAPRS*, Vol. 34, Part 3/W13, 6p.

Wagner, W., Hollaus, M., Briese, C., Ducic, V., 2008. 3D vegetation mapping using small-footprint full-waveform airborne laser scanners. *International Journal of Remote Sensing*, 29 (5), pp. 1433-1452.